An Introduction to Velocity-Map Imaging Mass Spectrometry (VMImMS)

James N. Bull, Jason W. L. Lee, Sara H. Gardiner, and Claire Vallance*

Chemistry Research Laboratory, Department of Chemistry, University of Oxford, 12 Mansfield Road, Oxford OX1 3TA, United Kingdom

*claire.vallance@chem.ox.ac.uk Tel: +44 (0)1865 275179

This account introduces a new variant of time-of-flight (ToF) mass spectrometry (MS), termed Velocity-Map Imaging Mass Spectrometry (VMImMS). While the ion abundances recorded in conventional ToF-MS measurements are highly useful for molecular quantification and structure determination, the final parent and fragment ion yields are largely blind to the dynamics of the processes in which the ions were formed inside the mass spectrometer. By recording the velocity distribution of each ion in tandem with the mass spectrum, not only can the details of the dissociative ionization dynamics be unravelled, but the extra dimensions of information can be used for enhanced molecular fingerprinting, separating contributions from ions with identical mass-to-charge ratio, and resolving components within mixtures, to name but a few examples. Measuring ion velocity distributions within a mass spectrometry measurement is not new, but incorporating imaging techniques developed within the reaction dynamics community provides vastly improved velocity resolution for all ions simultaneously in a single-stage instrument. This account provides an introduction to VMImMS outlines the fundamental instrumentation and detector requirements and the challenges associated with developing the method further, and details proof-of-concept work from our laboratory on a number of potential applications of the technique.

1. Introduction

The ionization processes employed in most types of mass spectrometry often lead to a considerable degree of fragmentation. Depending on the amount of energy deposited into the parent molecule, the degree of dissociation may be small, or the molecule may undergo a variety of different fragmentation processes, exhibiting a complex interplay between direct bond breaking and indirect dissociation mechanisms involving energy redistribution and often structural isomerisation. The particular combination of dynamical processes is determined by the electronic structure of the parent molecule, and probing these dynamics can therefore provide a means of molecular identification and quantification.

Conventional time-of-flight mass spectrometry (ToF-MS) probes one characteristic observable relating to the dissociation dynamics, namely the yield of each fragment ion produced following ionization. However, if instead of simply counting the total number of fragment ions of each mass, the detection step is able to resolve the ion velocities, it becomes possible to probe the detailed

dynamics of the fragmentation process, often at a quantum-state-resolved level[1,2]. The ion velocity distributions are a sensitive probe of the fragmentation dynamics, since they are determined by the forces acting on the fragments as they dissociate, and therefore by the topography of the molecular potential energy surface(s) over which the dissociation occurs. There are a number of ways in which fragment velocity distributions may be of use in mass spectrometry. For example, ions of identical *m*/*z* from different sources are indistinguishable in a conventional mass spectrum. However, if the dissociation dynamics leading to formation of the ions are significantly different, the individual contributions from multiple channels may be quantified on the basis of the velocity distributions of the respective ions.

To date, ToF mass spectrometer development has generally focused on improving mass resolution and ion throughput, as well as on incorporating soft ionization techniques for non-volatile samples, and improved hybridization in tandem or hyphenated techniques[3-14]. Many of these developments are driven by the requirements of researchers working in the fields of molecular biology and biochemistry. Methods such as matrix-assisted laser desorption ionization (MALDI) imaging, often referred to more generally as 'imaging mass spectrometry', have added spatial information to mass spectra, and are increasingly being used in areas such as tissue analysis for mapping lipids, peptides, and metabolites in biological samples[15-20]. However, none of these methods exploit the information contained in the fragment ion velocity distributions.

A limited amount of information on fragment ion velocity distributions can be obtained through the analysis of high-resolution ToF peak profiles[21]. Techniques such as mass-analysed ion kinetic energy spectrometry (MIKES)[22,23] allow fragment kinetic energy distributions to be measured for selected ions, though require a fairly complex experimental scheme involving scanning magnetic and electric sectors. While MIKES has been used with considerable success to resolve mixtures of components from complex samples, including volatile vapours from heated coal dust or natural products[24-27], the data acquisition and analysis is time consuming, and the kinetic energy resolution is low. Tandem mass spectrometry (MS/MS) similarly offers some capabilities for studying mixtures[14], though also requires a two-stage mass spectrometer.

This account outlines a new and developing implementation of ToF mass spectrometry, termed velocity-map imaging mass spectrometry (VMImMS)[1], which allows the complete velocity distribution for each ion to be measured in tandem with the mass spectrum. The technique is suited to target molecules with molecular masses of up to several thousand atomic mass units. In contrast to MIKES, images can be acquired for each *m*/*z* in a single-stage instrument with no requirement for prior knowledge of the ion flight times. As discussed above, from a chemical physics perspective, the additional information can be used to elucidate details of the ion fragmentation dynamics. However, at a simpler level it can also be used simply as a 'fingerprinting' method for the various fragment ions and dissociation channels. In the following, we provide an introduction to velocity-map imaging (VMI), outline the basic requirements for a practical mass spectrometer, and present three proof-of-concept examples illustrating the potential applications. The principles of velocity-map imaging (VMI) have been detailed previously in the European Journal of Mass Spectrometry in an account by Heck[28]; the present account considers the transition from using VMI as a technique for probing fundamental processes in chemical physics to more generalised applications in mass spectrometry.

2. Principles of velocity-map imaging

A velocity-map imaging mass spectrometer is essentially modified ToF instrument, in which the ToF ion optics are replaced with a VMI lens assembly, and the ion-counting or integrating detector is replaced with a position-sensitive detector[1]. In the chemical physics experiments for which VMI was originally developed, the molecule of interest is usually expanded in a molecular beam, which is then intersected by one or more laser beams to create ions. However, many other ion source configurations are possible. The VMI lens[29-32], which in its simplest form consists of three open (meshless) electrodes, projects the velocity vectors of the nascent ions formed in the ion source region along a ToF axis onto the position sensitive detector. By mapping ions formed with identical velocities onto the same point on the detector irrespective of their initial position, the velocity-mapping lens corrects for the blurring of the image that would otherwise occur due to the finite region in which ions are formed, i.e. the system behaves as if an ideal point source of ions has been achieved, greatly improving the velocity resolution. Figure 1 illustrates velocity-mapping of a number of ions contributing to a single *m/z* peak in a typical VMI set-up. We note that in the context of mass spectrometry, VMI detection immediately reveals whether the mass extraction is quantitative or whether there is discrimination against high-kinetic-energy ions. For example, quantitative detection has not been achieved if images extend beyond the edges of the detector.

A typical VMI detector, shown schematically in Figure 1, generally consists of a chevron pair of microchannel plates (MCPs) coupled to a fast phosphor screen[46]. The MCPs convert incoming ions into electron bursts, which excite luminescence in the phosphor. The spatial distribution of incoming ions is therefore converted into an optical image on the phosphor, which can be captured by a camera. The resulting image is a two-dimensional projection of the full three-dimensional velocity distribution for each *m/z*. The mass spectrum is obtained simultaneously by recording either the ion current across the MCPs, or an optical signal from the phosphor, as a function of time. The frame rates of most cameras limit acquisition to one ion *m/z* per ToF cycle, with mass selection achieved through time-gating of either the MCPs or an image intensifier within the camera. As will be detailed in Section 3.5, highly specialised cameras have been developed recently which allow images to be acquired for multiple ion *m/z* on each experimental cycle.

The radial coordinate of a velocity-map image is proportional to the velocity component of the ion in the image plane, while the angular coordinate reveals its scattering angle. When the velocity distribution has cylindrical symmetry, which is often the case in laser-based dissociation and ionization schemes, an inverse Abel or Hankel transform can be used to 'reinflate' the 2D projection into a 3D velocity distribution, and a slice through the centre of this distribution then contains all of the required dynamical information[32,39,40]. A variety of forward convolution and fitting methods have been developed for more complex cases. Further details and examples of the reconstruction procedure for small-molecule photoionization studies are available in the earlier account of Heck[28]. For applications in mass spectrometry, the quantity of greatest interest is usually the kinetic energy release (KER) distribution. This can be obtained by integrating the '2D slice' over the angular coordinate, and converting the speed axis into an energy axis.

There are a number of possible improvements to the simplest VMI lens design, which provide enhanced image resolution and other capabilities; for example 'slice imaging'[41,42,43] allows the '2D slice' referred to above to be measured directly, without the need for an Abel inversion. On-the-fly computational algorithms such as event counting[44] and 'megapixel imaging'[45] can also provide considerably enhanced velocity resolution. Detailed historical accounts of VMI as well as a summary of current state-of-the-art implementations can be found in a number of recent reviews[32-35].

VMI has been widely used for nearly two decades by the chemical physics community to study laser-induced dissociation dynamics and other fundamental chemical processes.[32-35] Most studies have involved small molecules containing between two to ten atoms, with the majority focusing on quantum-state-resolved investigations into the photofragmentation dynamics of diatomics and triatomics. As molecular size increases, so does the number and density of accessible states, providing efficient energy redistribution and relaxation processes.[21,36,37] This decreases the usefulness of the imaging dimension to some extent, but highly structured, and therefore information-rich, images have been observed even for relatively large chemical species (at least from a physical chemist's perspective) of twenty or more atoms.[38] Due to the large number of potential fragmentation channels for molecules with more than a few atoms, detailed quantum-state-resolved analysis is not generally possible, but the KER distributions of the fragments do still retain considerable information on the partitioning of energy between translational and internal degrees of freedom of the products.

When developing VMI for mass spectrometric applications, the instrumental requirements are somewhat different from those for fundamental chemical physics studies[1]. Universal ionization (i.e. ionization of all chemical species in the ionization volume) replaces laser-based quantum-state selective ionization processes; achieving high mass resolution becomes much more important when larger molecules are to be studied; and the ability to acquire multiple images within a given ToF cycle is necessary in order to allow data acquisition to occur on a reasonable experimental timescale – so-called multimass imaging.[2,38,47,48] It is emphasised that VMImMS is still in the very early stages of development, and faces a number of experimental challenges as it evolves from its origins in small-molecule fundamental chemical physics studies into a useful analytical technique.

3. Instrumentation

Assuming that the appropriate specifications can be met, a ToF velocity-map imaging mass spectrometer has potential applications both in fundamental ion physics studies and in small-molecule mass spectrometry. As noted above, the key requirements are to identify a suitable universal ionization technique for use with VMI, to achieve sufficiently high mass resolution for applications in analytical mass spectrometry with a reasonable throughput, and to develop detectors capable of multimass imaging at a reasonably high repetition rate. These requirements are considered in turn.

3.1 Universal ionization

A variety of universal ionization methods are in widespread use in mass spectrometry. These include electron impact ionization, fast-atom bombardment, electrospray ionization, and matrix-assisted laser desorption ionization[4]. Some of these methods (e.g. electron-impact ionization) induce considerable molecular fragmentation, while others are often combined with additional fragmentation methods in order to elucidate further details of molecular structure. Commonly-used fragmentation methods include collision-induced dissociation (CID), infrared multiphoton dissociation (IRMPD), electron capture dissociation (ECD), and UV photodissociation (UVPD). Ionization and fragmentation methods can be divided into two categories. The first includes methods such as electron impact ionization and UV or VUV photoionization, in which energy is deposited into the molecule in a short space of time, i.e. ideally shorter than one molecular vibration. Direct vertical ionization occurs, with considerable molecular fragmentation ensuing if the available energy exceeds the dissociation energies of one or more chemical bonds. Dissociation can be rapid (kinetic fragmentation) if repulsive states or highly excited electronic states are populated, and fragment kinetic energy distributions are often highly structured and unique to the parent molecule. The second category of fragmentation methods includes processes such as IRMPD and ECD, in which the molecule absorbs energy

gradually until one or more dissociative ionization thresholds are reached. There is ample time for energy to redistribute amongst the various molecular degrees of freedom, and as a result the fragment internal state and kinetic energy distributions are broad and unstructured, determined statistically by the Boltzmann distribution. Such 'thermodynamic' fragmentation processes are less suited to interrogation via VMI methods since the KER distributions tend to peak at very low energies, show little or no structure, and may be very similar for different fragment ions.

Ideally then, VMImMS requires a 'hard' and essentially instantaneous ionization mechanism, which deposits a significant amount of energy into the target molecule in excess of the ionization potential, yielding molecular fragmentation. In contrast, ‘soft’ ionization mechanisms only deposit a small excess of energy above the ionization potential, resulting in a small degree of fragmentation and potentially a high abundance of parent ion. While a number of existing universal ionization methods potentially satisfy the required criteria for VMImMS, the two that are currently being investigated in our laboratory are electron-impact ionization and ultraviolet (UV) or vacuum ultraviolet (VUV) photoionization.

Electron impact represents an ideal dissociative ionization mechanism for VMI studies in that for electron energies significantly in excess of the ionization potential, numerous highly excited and dissociative electronic states of the ion are accessed, often leading to extensive fragmentation via numerous dissociation channels[1,49,50]. Channels involving loss of more than one electron are also energetically accessible once the electron energy exceeds the double or triple ionization threshold of the molecule, and tend to result in direct and rapid fragmentation. The primary difficulty in implementing electron-impact ionization in tandem with VMI is tuning the electron beam in order to achieve simultaneous optimisation of velocity mapping and mass focusing. This is discussed further in Section 3.2.

Single-photon and multiphoton ionization methods have both been used extensively in mass spectrometry and are the subject of several reviews[4,51-56], including a previous account in the present journal by Weckhardt *et al*[57]. The photon energies required to exceed the ionization energies of most molecules are generally achievable only with synchrotron radiation or specialised vacuum ultraviolet laser sources. Here the focus is on high-powered laboratory sources, which usually involve third-harmonic generation from the 355 nm frequency-tripled output of a Nd:YAG laser or frequency-doubled output from a dye laser.[51-53] Third-harmonic generation can be achieved by passing the radiation through a phase-matched mixture of inert gases, allowing wavelengths of around ~118 nm (10.51 eV) to be accessed in the case of the Nd:YAG source[58]. Such energies are only just in excess of the first ionization threshold for most molecules, and single-photon ionization is therefore often considered to be a relatively 'soft' ionization method which does not lead to a great deal of parent ion fragmentation. Single photon ionization provides an ideal approach when a high population of parent ion is desirable, but does not lead to the relatively high degree of fragmentation desirable for molecular fingerprinting via VMI. The same is not true of multiphoton ionization and fragmentation methods. Depending on the photon energies employed, ionized fragments suitable for VMI analysis may be formed via a variety of mechanisms: (i) Single-photon ionization of the parent molecule followed by fragmentation of the parent ion following absorption of one or more additional photons; (ii) multi-photon ionization of the parent molecule to yield a parent ion with sufficient internal energy to undergo fragmentation; or (iii) photofragmentation of the neutral parent molecule followed by single-photon or multiphoton ionization of one or more fragments. In the context of mass spectrometry, the fragmentation patterns observed in (i) and (ii) yield structural information on the parent molecular ion, while (iii) yields structural information on the neutral. In contrast to electron-impact ionization, photoionization total and partial ionization cross sections are generally not well

characterised, and are not easily predicted on the basis of physical models. This complication, especially for multiphoton processes, can make comparisons between mass spectra of different species very difficult. A further experimental complication arises from the fact that the relative contributions from different multiphoton processes are also highly sensitive to fluctuations in laser intensity.

By taking advantage of absorption resonances, photon-based ionization schemes offer a degree of control over the ionization process that is not available using (collision-like) electron-impact methods. For example, with sufficient knowledge of the relevant spectroscopy, resonance-enhanced multiphoton ionization (REMPI) allows small molecules to be ionized with selectivity down to the quantum-state-resolved level. While this is generally not of great value in mass spectrometry studies, it can be extremely useful in chemical dynamics studies when attempting to unravel the dissociation dynamics associated with the various energetically accessible fragmentation channels.[35]

As noted previously, conventional IRMPD methods that lead to 'statistical' fragmentation are not well suited to VMI analysis. However, it has been shown that high-power and ultra-short femtosecond laser pulses (kHz repetition rates) can provide a rather effective universal ionization source[4, 56,59 ,60]. The intense electric field of the pulse leads to very rapid dissociative ionization rather than generation of an excited state of the neutral. The resulting fragmentation can be similar to electron impact. Unfortunately, femtosecond laser systems are complex and expensive, rendering their use impractical for routine analytical applications at this time.

3.2 Time-of-flight or *m*/*z* resolution

A reasonable 'end goal' for a VMImMS instrument is to achieve a mass resolution similar to that of a commercial ToF instruments used to analyse small to medium-sized molecules. Such instruments typically achieve a mass resolution ($m/\Delta m$) of several thousand to tens of thousands. The ultimate time, and therefore mass, resolution of a VMImMS instrument is determined by a number of factors, which will be considered in turn.

The VMI optics used in chemical dynamics studies have been optimised for maximum velocity resolution, rather than for high ToF (or m/z) resolution, and as such are best used only for analytes with masses up to a few hundred atomic mass units. Simultaneously optimising both velocity resolution and mass resolution is challenging, but efforts are currently underway to design next-generation ion optics that achieves both high mass and high velocity resolution. It has recently been shown that mass resolutions of several thousand are possible in combination with imaging when employing various pulsed extraction schemes.[61,62]

An important factor influencing the achievable mass resolution is the extent of the ionization region along the ToF axis. When laser ionization methods are used, it is straightforward to focus the laser down to a spot size of a few hundred microns. However, achieving a tightly focused ionizing beam is more challenging in the case of electron ionization, with space-charge repulsion limiting the achievable spot size and/or beam density.[6,49] Achieving good focusing of an electron beam also requires that the ionization volume is well shielded from external electric or magnetic fields, including any fields arising from the ion optics of the mass spectrometer. These considerations are common to both imaging and non-imaging variants of ToF mass spectrometry.

The time response of the ion detector is another key factor in determining the overall time resolution of the spectrometer. As noted previously, the detectors used in most VMI experiments consist of a pair of microchannel plates coupled to a phosphor screen. While the MCPs can have

response times on the order of hundreds of picoseconds, the 95% decay lifetime of the P47 phosphor used in most detectors is around 120 ns. This places severe limitations on the achievable mass resolution. Some faster phosphors are currently commercially available, but suffer from very low brightness, which makes them poorly suited for imaging applications. It is evident that if MCP-phosphor based detectors are to be used, there is a need for new fast phosphors with decay lifetimes on the order of a few nanoseconds that offer both high brightness and greatly improved time resolution.

The final factor determining the mass resolution is the time response of the camera used to capture images from the phosphor screen. This will be considered in Section 3.5. It is also worth noting that for applications in which very few ions are generated on each ToF cycle (generally less than or equal to one ion per *m/z*), an alternative detection arrangement comprising a pair of MCPs coupled to a delay line anode can offer time resolutions limited only by the MCP response time – note that MCP dead times can be on the order of milliseconds under high gain conditions[63].

3.3 Throughput

The ion throughput is a key design parameter for any mass spectrometer, since a high throughput minimises the time required in order to acquire a mass spectrum with a given signal-to-noise ratio. The throughput is determined by both the number of ions detected on each time of flight cycle, and the repetition rate of the instrument, i.e. the number of ToF cycles per second. Commercial ToF instruments typically operate at repetition rates of several kHz, limited only by the ~200 μs arrival time distribution of the ions under normal operating conditions[6,7]. High throughput becomes especially important for a applications in which the spectrometer is coupled to a chromatographic technique (e.g. HPLC-MS or GC-MS), as a given component may take only a few seconds to elute, requiring a mass spectrum to be acquired with sufficient signal-to-noise ratio on this timescale.

While achieving a high ion throughput is desirable for any ToF instrument, it is especially advantageous for VMImMS. Instead of simply recording the total ion signal as a function of time, *t*, a VMImMS instrument resolves the signal at each *m/z* along a pair of velocity coordinates, so that the signal *S* is three-dimensional, $S(x,y,t)$ rather than one-dimensional, $S(t)$. Achieving a given signal-to-noise ratio for this three-dimensional signal requires the detection of a much larger number of ions than for the conventional one-dimensional ToF signal. Because in almost all mass spectrometry applications it is only the KER distribution of the ions that is required, which is acquired by integrating over the angular coordinate of the image, the situation is not quite as bad as might initially be anticipated. However, if *N* data points are wanted in the KER distributions, as a rule of thumb it will be necessary to detect at least *N* times more ions than in a simple ToF measurement. The number of data points required in order to describe the KER distributions adequately is often molecule-dependent, with narrow KER distributions requiring fewer data points than broad distributions.

One approach to improving ion throughput is to improve the detection efficiency. At present, this is determined largely by the open area ratio (OAR) of the microchannel plates assuming high-gain operation. In simple terms, the OAR is the percentage of the MCP surface made up by the pores within which charge multiplication occurs. Most commercially available MCPs have, at best, around 50-60% detection efficiency under high gain conditions, in line with their OAR – see for example reference 64. There have been a number of recent reports of MCPs employing tapered channels to achieve an OAR of greater than 90%, which immediately provides almost a factor of two improvement in detection efficiency under typical operating conditions[65,66]. Assuming they pass

consumer tests of reliability and robustness, these newer MCPs are in many instances likely to be adopted as a new standard over the next few years.

While improving the detection efficiency is very important for VMImMS applications, at present the primary factor limiting the ion throughput is the readout speed of the camera used to capture the images. Traditional 'video rate' CCD cameras read out at around 30 to 50 Hz. Newer scientific cameras can achieve frame rates of hundreds or even thousands of Hz, but there is still some way to go before readout rates for imaging mass spectrometry are competitive with the 20 to 30 kHz data acquisition cycles of conventional ToF instruments. This is only to be expected, as the volume of data that must be transferred and stored is many orders of magnitude higher in an imaging experiment. While data transfer and handling capabilities are constantly being advanced, there is certainly plenty of scope for further improvement in this area. The capabilities of new state-of-the-art time-resolved imaging sensors will be discussed briefly in Section 3.5.

3.4 Dynamic range

In the ToF dimension, VMImMS is subject to the same dynamic range considerations as a conventional ToF instrument. If the mass spectrum is acquired via the total ion current recorded across the MCPs then the dynamic range in the ToF spectrum is determined largely by the number of bits used to digitise the data, provided moderate gain conditions and no detector saturation. In an imaging experiment, one also has to consider the dynamic range in the imaging or ion KER dimensions. As noted earlier, fragment ion velocity distributions are determined by the dynamics of the fragmentation process in which the ions were formed, and can therefore show considerable variation. Non-statistical dissociations and double ionizations for molecules of several hundred to several thousand atomic mass units may produce KER distributions extending out to ~10 eV, while statistical dissociations produce KER distributions spanning only around 0.1 eV to 2 eV.[1,37] The imaging detectors used in most VMImMS instruments are 40 mm to 75 mm in diameter, with typical flight tube lengths of around 0.5 m. Recording KER distributions extending out to 10 eV for masses of between ten and several hundred atomic mass units requires extraction potentials of tens of kilovolts. Such high acceleration potentials have the unfortunate consequence of compressing the entire ToF profile into a few tens of microseconds, reducing the achievable mass resolution. In order to achieve both imaging of high KER ions and ToF dispersion over several hundred microseconds, further developments in ion optics design are required in order to provide improved zooming and focusing capabilities suitable for VMImMS.[67,68]

3.5 Fast time-resolved imaging detectors

As noted earlier, if a VMImMS instrument utilizes a MCP-phosphor detector, then the ion images generated on the phosphor screen must be captured by a camera. VMI instruments have traditionally utilized charge-coupled-device (CCD) cameras, which tend to be inexpensive and can provide high resolution (megapixel) images. Unfortunately, as noted in Section 3.3, most commercially available CCD cameras are limited to an acquisition rate of tens of Hertz. This means that only one predefined *m/z* can be imaged on each ToF cycle, which is usually selected either by time-gating the potentials applied to the MCPs so that they are only active over the arrival time window of the ion of interest, or by time-gating an image intensifier within the camera itself. This has not been a significant limitation in small-molecule laser-based VMI studies, since imaging of one fragment is often sufficient to obtain most of the desired information on the process under study, and experimentalists are willing to devote several hours to acquiring such an image. In addition, such laboratory experiments are generally limited to repetition rates of 10 or 20 Hz by the fixed repetition rates of the laser systems employed

rather than by the camera. In principle, time-gating of the detector at even kHz repetition rates or higher would allow images from many experimental cycles to be summed within a single exposure of a conventional CCD camera. However, this procedure does not address the problem of acquiring images simultaneously for more than one *m/z* (multimass imaging). In addition, time-gating requires prior knowledge of the ion arrival times of interest.

Several high-speed CCD cameras are available commercially with frame rates of 1 MHz or higher; however these cameras typically have low resolution, and it is usually only possible to store a limited number of frames at these high frame rates before they must be read out relatively slowly to a computer. Though frame rates in the kHz and MHz ranges address issues relating to experimental repetition rates, they still do not allow for multimass detection within a single ToF cycle. Some limited success in multimass imaging has been achieved using specialised frame-transfer CCD cameras, which store multiple frames on-chip before readout,[2] but this approach is only suitable for imaging a relatively small number of ions on each cycle, whose arrival times have already been well characterised. The framing technology is not infinitely scalable, as increasing the number of images that can be stored on-chip is achieved at the expense of a reduction in the light-sensitive area within each pixel, and therefore a reduction in detection sensitivity.

More promising are recent developments in intelligent CMOS pixel technology, which allows for on-pixel logical operations and signal processing.[48,69,70] Two sensors are of particular note: the TimePix/MediPix sensor, developed at CERN[69,71,72]; and the PImMS (Pixel Imaging Mass Spectrometry) sensor[38,73], developed in Oxford. Though the details of the two sensors differ, they share the feature that each pixel is able to record ion arrival times independently. The TimePix sensor consists of a 256×256 array of 55×55 μm pixels, and four sensors can be tiled together to yield a 512×512 pixel 'quad' sensor.[74] The TimePix sensor detects charged particles directly, rather than detecting light from a phosphor screen, and in a VMI context can been used in isolation to record electron hits, and in combination with a pair of MCPs to record ion velocity distributions.[75] Each pixel can be programmed to run in one of three modes during an acquisition cycle, recording either the total number of incident particles, the arrival time of the first incident particle (with a time resolution of around 10 ns), or the 'time over threshold', a measure of the particle energy. The second, 'TimePix', mode is of most use for applications in VMImMS. Since each pixel can only register one ion arrival time per acquisition cycle, with later ions not being detected, care must be taken to run the experiment under conditions such that this is sufficient to detect all ions, placing a limit on the maximum signal level. The appropriate signal level must therefore be determined in advance before quantitative mass spectra or reliable KER distributions can be extracted. Multimass imaging has been reported using TimePix.[76]

The PImMS sensor is configured to detect light, and in a VMImMS instrument is coupled via a lens to detect light from the phosphor screen of the imaging detector. During each acquisition cycle, each pixel can record arrival times of up to four ions with a time resolution of 12.5 ns. Simulations have indicated that under typical operating conditions within a VMImMS instrument, four memory registers per pixel is sufficient to detect over 95% of ions, overcoming potential problems associated with 'shadowing' in the images of heavier ions inherent in TimePix due to inactivation of pixels that have already detected lighter ions. The first generation PImMS1 sensor comprises a 72×72 pixel array, and has already been demonstrated in a number of different time-resolved imaging applications, including imaging mass spectrometry, multimass imaging, and other areas.[38,48,77] The second generation PImMS2 sensor has an increased resolution of 324×324 pixels, and is currently in the testing phase. It is noted at this point that there are a number of other sensor technologies that may have the potential to be adapted for imaging mass spectrometry.[48,69,70]

In both framing CCDs and intelligent CMOS detectors, the readout to computer memory occurs at end of each acquisition cycle, and the achievable overall acquisition rate therefore depends on a combination of readout interface speed and firmware-based processing to reduce data transfer requirements. The current generation TimePix sensor can operate at readout rates of between 30 and 1000 Hz, the PImMS1 sensor can currently operate at readout rates of up to ~300 Hz (via a USB2 interface)[‡], while the larger PImMS2 sensor can readout at ~15 Hz. Improvements of a factor of ten to one hundred for the PImMS1 sensor would bring it to within comparable repetition rates of commercial ToF instruments. However, the increased volume of data in an imaging experiment relative to a simple ToF measurement makes it extremely challenging to achieve comparable data rates, and this is therefore an active area for research and development.

It is also appropriate at this point to mention an alternative to fast cameras, namely the delay-line anode[63]. Such a device is placed immediately behind the MCPs of an imaging detector, in place of the phosphor screen, and consists of two or more wires wound along the *x* and *y* coordinates (and sometimes one or more diagonal coordinates), respectively. An electron burst incident on the anode results in a current pulse in both directions along the *x* and *y* wires, and by recording the arrival times of the current pulse at each end of the two wires, the position of the incident ion can be triangulated. The arrival time of the ion is determined from the current pulse recorded across the MCP, and in the best detectors can be pinpointed to within around 25 ps. The downside of such detectors is that typically only one ion can be detected at a time across the whole detector, with a 'dead time' of at least several nanoseconds after each detection event. Delay-line detectors are therefore ideally suited for experiments that run at high repetition rates of tens to hundreds of kHz, but with very low signal levels on each experimental cycle. Delay line anodes can be used directly for multimass imaging.[78]

As a final consideration, the extent to which features in the KER distribution can be resolved is usually determined by the number of pixels in the sensor array (i.e. the camera usually determines the resolution, rather than the performance of the ion optics or the ion detector). While small molecules often display considerable fine structure in their fragment KER distributions ideally requiring an array of 1000×1000 or so pixels, the features for larger molecules tend to be much broader, and a sensor with several hundreds of pixels along each dimension is sufficient. Both the PImMS and TimePix sensors have sufficient spatial and time resolution for multimass imaging, though data acquisition speed is an area for improvement.

4. Example applications of velocity-map imaging mass spectrometry

This section briefly outlines three recent ion physics studies performed in our laboratory to illustrate the usefulness of the extra dimensions of information available through VMI. Data for the first example was acquired using a laser-based VMI apparatus first detailed in Hopkins *et al*.[79], and data for the latter two was acquired using an electron-impact-based instrument recently detailed in Bull *et al*.1. Further details on the first example can be found in a recent publication by Gardiner et al[80].

4.1 Molecular fingerprinting using laser ionization and fragmentation

The first example illustrates the highly distinctive images that can arise following laser ionization and fragmentation of two similar molecules, in this case ethyl iodide (C_2H_5I) and ethyl bromide (C_2H_5Br). The molecules were each prepared in a molecular beam and irradiated by 118 nm and 355 nm laser pulses, with the former generated by frequency tripling the 355 nm third harmonic of a Nd:YAG laser in a phase-matched mixture of inert gases.[51-53] The 118 nm (10.51 eV) photon ionized the neutral molecules to produce $C_2H_5Br^+$ (with isotopologues at m/z = 108 and 110) or $C_2H_5I^+$ (m/z = 156), with

subsequent absorption of a 355 nm photon leading to fragmentation of the parent ion. Mass spectra and corresponding velocity-map images for the two molecules are shown in Figure 3(a) and 3(b), respectively. All of the images exhibit some degree of angular anisotropy, due to the anisotropic interaction between the linearly polarised 355 nm photon and the transition dipole associated with excitation of the parent ion to a dissociative state.[81] The modest energy provided by the 355 nm photon leads to relatively limited fragmentation, yielding ion signals at m/z = 27 ($C_2H_3^+$), 28 ($C_2H_4^+$), and 29 ($C_2H_5^+$) and, in the instance of C_2H_5I, atomic I^+ at m/z = 127. The different fragments have highly distinctive images, as do the identical fragments arising from the two different parent molecules, demonstrating the potential utility of 118 nm radiation combined with VMImMS for molecular fingerprinting.

FIGURE 5 NEAR HERE

4.2 Distinguishing ions of identical mass-to-charge ratio

One of the most useful features of the KER distributions extracted from velocity-map images is the immediate distinction between parent ions and daughter/fragment ions. Parent ions exhibit a near zero KER, since loss of one electron does little to perturb the velocity vector of the parent molecule. In contrast, the KER distributions of the daughter ions exhibit broader KER distributions with features characteristic of their respective local electronic environments in the parent molecule. The ability to distinguish parent and daughter ions in this way was recently demonstrated in a study from our laboratory in which VMImMS was used to resolve two contributions to the mass peak at m/z = 14 following electron impact ionization of N_2.[1] Both the doubly charged N_2^{2+} ion and the singly charged N^+ ion contribute to signal at this m/z ratio. KER distributions for m/z = 28 and 14, both relevant to the discussion below, are given in Figure 3.

Partial ionization cross-sections for m/z = 14 and 28 (N_2^+) can be extracted from the mass spectrum, with the visualisation of the ion velocity distribution via VMI proving useful in ensuring that all ions are detected i.e. that a 'quantitative' mass spectrum has been recorded. The N_2^+ ion at m/z = 28 shows the characteristic near-zero KER distribution of a parent ion, as explained above, while the daughter ion peak at m/z = 14 reveals a much broader distribution. The N_2^{2+} and N^+ contributions to the peak at m/z =14 can be disentangled through fitting of the corresponding image. The N_2^{2+} contribution must exhibit a KER distribution essentially identical to that of the N_2^+ ion, since loss of two electrons still does little to perturb the velocity vector of the parent molecule. The remaining portion of the image arises from various N^+ dissociation channels, which can be assigned to dissociation from different excited states of N_2^+ and N_2^{2+} through consideration of the appropriate potential energy surfaces. Further details will be given in a future publication. Comparison of the partial ionization cross-sections determined using these methods with results obtained previously in experiments on the $^{14}N^{15}N$ isotopologue reveals close agreement.[78] In the present case, the data show that with 100 eV electrons, 9±1% of the ions produced at m/z = 14 can be attributed to N_2^{2+} ions, and 91±1% to N^+ ions.

It is acknowledged that the N_2 system represents a simple and idealized case. However, the approach is certainly not limited to resolving X^+ and X_2^{2+} ions, and can be used for any system in which the ions to be distinguished have sufficiently different KER distributions.

FIGURE 3 NEAR HERE

4.3 Resolving components in simple mixtures

The final example illustrates the use of a simple linear fitting algorithm to resolve multiple components within a simple mixture using both the mass spectrum and the extra dimension of information available using VMI. The mixture used for this demonstration consists of three alcohols: ethanol, propan-1-ol, and propan-2-ol. Electron-impact mass spectra for each alcohol at the fixed energy of 70 eV are shown in Figure 5 (left), and the corresponding KER distributions for three selected *m*/*z* values, corresponding to $C_2H_5O^+$, CH_3O^+ and CH_3^+ ions, respectively, are shown in Figure 5 (right). Fragmentation of the three alcohols yields many ions in common; for example, parent ions of ethanol are isobaric with fragment ions from the heavier two alcohols. This would make it difficult to resolve the relative contributions from the various molecules based purely on fitting a linear combination of mass spectra. However, close inspection of the fragment ion KER distributions reveals characteristic features that allow the various contributions to each ion signal to be quantified. In ethanol, for example, the $C_2H_5O^+$ fragment exhibits a KER distribution almost identical to that of the parent ion, since the recoil imparted to this fragment by loss of one hydrogen atom is small. In contrast, the KER distribution for the same ion produced from either of the propanol isomers is broader, since it involves cleavage of a C-C bond. The CH_3O^+ ions produced from each of the alcohols possess broadly similar KER distributions, but still show subtle differences in the extent of the high energy 'tail'. Finally, the CH3+ ion exhibits a bimodal KER distribution for all three parent ions, but with clear differences in the relative intensities of the two peaks. The peak at 4.4 eV almost certainly arises from a direct non-statistical dissociation process.

As a result of the characteristic KER distributions for the various fragment ions, if the mass spectra are fitted at the same time as the KER distributions, the relative concentrations of each component within the mixture can be determined reliably to within a few percent. In this example, the KER distributions for each component first need to be measured individually in order to extract 'basis functions' to be used in the fitting procedure. Thus, similar to traditional EI mass spectra, many applications of VMImMS for identification and characterization will benefit from comparisons with certified databases or libraries of mass spectra and KER distributions. In the general mixtures case, a VMImMS study would not consider just three ions, as in the simple example presented here, but would instead consider a linear combination of KER distributions from *all* sufficiently abundant *m*/*z* peaks present in the mass spectrum of the mixture. The inclusion of KER distributions for all ions is especially important as molecular size increases and the fragmentation becomes increasingly 'thermodynamic' or 'statistical' in nature.

FIGURE 4 NEAR HERE

It should be noted that both MIKES and tandem ToF-ToF can provide limited information on mixtures, as noted in the Introduction; however this example has demonstrated a *single stage* mass spectrometric method in which component contributions are resolved.

5. Conclusions

This account has introduced the technique of velocity-map imaging mass spectrometry (VMImMS), outlined the basic requirements of a practical VMImMS instrument, identified a number of areas in which further development is required, and demonstrated several potential applications of VMImMS through a series of simple examples. It is acknowledged that the technique is still in the early stages of development, and faces a number of instrumental and technological challenges before it is ready for widespread application in the analytical sciences. However, if these challenges can be overcome, the

technique promises a number of enhancements to ToF mass spectrometry measurements, for example: a reliable methodology for distinguishing parent and fragment ions; the ability to quantify relative contributions from identical ions formed via different fragmentation channels; measurement of accurate partial ionization cross sections; direct analysis of mixtures in a single-stage instrument; and higher-confidence differentiation of species yielding similar fragmentation patterns, e.g. isomers. Throughout the article, VMImMS has been considered as a single-stage mass spectrometric method. However, there is no reason why it could not be incorporated into the second stage of a tandem mass spectrometer, thereby allowing the fragmentation dynamics of mass-selected ions to be probed in detail.

Acknowledgments

Funding is acknowledged from Marie Curie Initial Training Network 238671 ‘ICONIC’, the EPSRC Programme Grant EP/G00224X/1, and ERC Starting Independent Research Grant 200733. The first two sources have provided Postdoctoral Fellowships for JNB and the second has provided a Ph.D. stipend for JWLL. We also thank Renato Turchetta, Andrei Nomerotski, Mark Brouard, Richard Nickerson, Jaya John John, and all other members of the PImMS fast image sensor collaboration. Some of the work described here is subject to a patent held by ISIS Innovations Ltd. (UK patent number 0724295.1; International patent PCT/GB2008/004085).

1. J. N. Bull, J. W. L. Lee and C. Vallance, “Quantification of ions with identical mass-to-charge (m/z) ratios by velocity-map imaging mass spectrometry”, *Phys. Chem. Chem. Phys.* **15**, 13796 (2013). doi: 10.1039/C3CP52219A

2. M. Brouard, E. K. Campbell, A. J. Johnsen, C. Vallance, W. H. Yuen and A. Nomerotski, “Velocity map imaging in time of flight mass spectrometry”, *Rev. Sci. Instrum.* **79**, 123115 (2008). doi: 10.1063/1.3036978

3. F. W. McLafferty, “A Century of Progress in Molecular Mass Spectrometry”, *Annu. Rev. Anal. Chem.* **4**, 1 (2011). doi: 10.1146/annurev-anchem-061010-114018

4. L. Burlingame, R. K. Boyd and S. J. Gaskell, “Mass Spectrometry”, *Anal. Chem.* **70**, 647R (1998). doi: 10.1021/a1980023+

5. S. A. McLuckey and J. M. Wells, “Mass Analysis at the Advent of the 21st Century”, *Chem. Rev.* **101**, 571 (2001). doi: 10.1021/cr990087a

6. C. Weickhardt, F. Moritz and J. Grotemeyer, “Time-of-flight mass spectrometry: State-of the-art in chemical analysis and molecular science”, *Mass Spectrom. Rev.* **15**, 139 (1996). doi: 10.1002/(SICI)1098-2787(1996)15:3<139::AID-MAS1>3.0.CO;2-J

7. M. Guilhaus, D. Selby and V. Mlynski, “Orthogonal acceleration time-of-flight mass spectrometry”, *Mass Spectrom. Rev.* **19**, 65 (2000). doi: 10.1002/(SICI)1098-2787(2000)19:2<65::AID-MAS1>3.0.CO;2-E

8. F. Xian, C. L. Hendrickson and A. G. Marshall, “High Resolution Mass Spectrometry”, *Anal. Chem.* **84**, 708 (2012). doi: 10.1021/ac203191t

9. F. W. McLafferty, “Tandem Mass Spectrometry”, *Science* **214**, 280 (1981). doi: 10.1126/science.7280693

10. F. W. McLafferty, “Tandem Mass Spectrometry: from Infancy to Maturity in Twenty-five Years”, *Org. Mass Spectrom.* **28**, 1403 (1993). doi: 10.1002/oms.1210281208

11. J. W. Hager, “Recent trends in mass spectrometer development”, *Anal. Bioanal. Chem.* **378**, 845 2004. doi: 10.1007/s00216-003-2287-1

12. J. D. Williams and D. J. Burinsky, “Mass spectrometric analysis of complex mixtures then and now: the impact of linking liquid chromatography and mass spectrometry”, *Int. J. Mass Spectrom.* **212**, 111 (2001). doi: 10.1016/S1387-3806(01)00460-2

13. F. W. Crow, K. B. Tomer and M. L. Gross, “Mass resolution in mass spectrometry/mass spectrometry”, *Mass Spectrom. Rev.* **2**, 47 (1983). doi: 10.1002/mas.1280020103

14. R. A. Yost and D. D. Fetterolf, “Tandem mass spectrometry (MS/MS) instrumentation”, Mass Spectrom. Rev. 2, 1 (1983). doi: 10.1002/mas.1280020102

15. J. D. Watrous and P. C. Dorrestein, “Imaging mass spectrometry in microbiology”, Nature Rev. Microbio. 9, 683 (2011). doi: 10.1038/nrmicro2634

16. S. S. Rubakhin, J. C. Jurchen, E. B. Monroe and J. V. Sweedler, “Imaging mass spectrometry: fundamentals and applications to drug discovery”, Drug Discovery Today 10, 823 (2005). doi: 10.1016/S1359-6446(05)03458-6

17. L. A. McDonnell and R. M. A. Herren, “Imaging Mass Spectrometry”, Mass. Spectrom. Rev. 26, 606 (2007). doi: 10.1002/mas.20124

18. D. S. Cornett, M. L. Reyzer, P. Chaurand and R. M. Caprioli, “MALDI imaging mass spectrometry: molecular snapshots of biochemical systems”, Nat. Meth. 4, 828 (2007). doi: 10.1038/NMETH1094

19. K. Schwamborn and R. M. Caprioli, “Molecular imaging by mass spectrometry - looking beyond classical histology”, Nature Rev. Cancer 10, 639 (2010). doi:10.1038/nrc2917

20. Rompp and B. Spengler, “Mass spectrometry imaging with high resolution in mass and space”, Histochem. Cell Biol. 139, 759 (2013). doi: 10.1007/s00418-013-1097-6

21. J. Laskin and C. Lifshitz, “Kinetic energy release distributions in mass Spectrometry”, J. Mass. Spectrom., 36, 459 (2001). doi: 10.1002/jms.164

22. J. H. Beynon, F. M. Harris, B. N. Green and R. H. Bateman, “Design of a Mass and Ion Kinetic Energy Spectrometer for Organic Chemical Work”, Org. Mass Spectrom. 17, 55 (2005). doi: 10.1002/oms.1210170202

23. J. H. Beynon, R. G. Cooks, J. W. Amy, W. E. Baitinger and T. Y. Ridley, “Design and Performance of a Mass-analyzed Ion Kinetic Energy (MIKE) Spectrometer”, Anal. Chem. 45, 1023A (1973). doi: 10.1021/ac60334a763

24. T. L. Kruger, J. F. Litton and R. G. Cooks, “Analysis of Mixtures by Ion Kinetic Energy Spectrometry”, Anal. Lett. 9, 533 (1976). doi: 10.1080/00032717608059118

25. T. L. Kruger, J. F. Litton, R. W. Kondrat and R. G. Cooks, “Mixture Analysis by Mass-Analyzed Ion Kinetic Energy Spectrometry”, Anal. Chem. 48, 2113 (1976). doi: 10.1021/ac50008a016

26. D. Zakett, V. M. Shaddock and R. G. Cooks, “Analysis of Coal Liquids by Mass-Analyzed Ion Kinetic Energy Spectrometry”, Anal. Chem. 51, 1849 (1979). doi: 10.1021/ac50047a054

27. R. G. Cooks, R. W. Kondrat, M. Youssefi and J. L. McLaughlin, “Mass-Analyzed Ion Kinetic Energy (MIKE) Spectrometry and the Direct Analysis of Coca”, J. Ethnopharm. 3, 299 (1981). doi: 10.1016/0378-8741(81)90060-X

28. J. R. Heck, “Throwing light on molecules falling apart: photofragment imaging,” *Eur. Mass Spectrom.*, **3**, 171 (1997). doi: 10.1255/ejms.36

29. D. W. Chandler and P. L. Houston, “Two-dimensional imaging of state-selected photodissociation products detected by multiphoton ionization”, J. Chem. Phys. 87, 1445 (1987). doi: 10.1063/1.453276

30. T. J. B. Eppink and D. H. Parker, “Velocity map imaging of ions and electrons using electrostatic lenses: Application in photoelectron and photofragment ion imaging of molecular oxygen”, Rev. Sci. Instrum. 68, 3477 (1997). doi: 10.1063/1.1148310

31. D. H. Parker and A. T. J. B. Eppink, “Photoelectron and photofragment velocity map imaging of state-selected molecular oxygen dissociation/ionization dynamics”, J. Chem. Phys. 107, 2357 (1997). doi: 10.1063/1.474624

32. B. J. Whitaker, Imaging in Molecular Dynamics, Cambridge University Press, 2003.

33. A. I. Chichinin, K. H. Gericke, S. Kauczok and C. Maul, “Imaging chemical reactions – 3D velocity mapping”, Int. Rev. Phys. Chem. 28, 607 (2009). doi: 10.1080/01442350903235045

34. S. J. Greaves, R. A. Rose and A. J. Orr-Ewing, “Velocity map imaging of the dynamics of bimolecular reactions”, Phys. Chem. Chem. Phys. 12, 9129 (2010). doi: 10.1039/C001233E

35. M. N. R. Ashfold, N. H. Nahler, A. J. Orr-Ewing, O. P. J. Vieuxmaire, R. L. Toomes, T. N. Kitsopoulos, I. A. Garcia, D. A. Chestakov, S.-M. Wu and D. H. Parker, “Imaging the dynamics of gas phase reactions”, Phys. Chem. Chem. Phys. 8, 26 (2006). doi: 10.1039/B509304J

36. H. M. Rosenstock, M. B. Wallenstein, A. L. Wahrhaftig and H. Eyring, “Absolute Rate Theory for Isolated Systems and the Mass Spectra of Polyatomic Molecules”, Proc. Nat. Acad. Sci. 38, 667 (1952). doi: 10.1073/pnas.38.8.667

37. G. E. Busch and K. R. Wilson, “Triatomic Photofragment Spectra. I. Energy Partitioning in NO2 Photodissociation”, J. Chem. Phys. 56, 3626 (1972). doi: 10.1063/1.1677740

38. A. T. Clark, J. P. Crooks, I. Sedgwick, R. Turchetta, J. W. L. Lee, J. J. John, E. S. Wilman, L. Hill, E. Halford, C. S. Slater, B. Winter, W. H. Yuen, S. H. Gardiner, M. L. Lipciuc, M. Brouard, A. Nomerotski and C. Vallance, “Multimass Velocity-Map Imaging with the Pixel Imaging Mass Spectrometry (PImMS) Sensor: An Ultra-Fast Event-Triggered Camera for Particle Imaging”, J. Phys. Chem. A 116, 10897 (2012). doi: 10.1021/jp309860t

39. V. Dribinski, A. Ossadtchi, V. A. Mandelshtam and H. Reisler, “Reconstruction of Abel-transformable images: The Gaussian basis-set expansion Abel transform method,” *Rev. Sci. Instrum.*.**73**, 2634 (2002). doi: 10.1063/1.1482156

40. L. M. Smith and D. R. Keefer, “Abel inversion using transform techniques,” *J. Quant. Spectrosc. Transfer*, **39**, 367 (1988). doi: 10.1016/0022-4073(88)90101-X

41. C. R. Gebhardt, T. P. Rakitzis, P. C. Samartzis, V. Ladopoulos and T. N. Kitsopoulos, “Slice imaging: A new approach to ion imaging and velocity mapping”, Rev. Sci. Instrum. 72, 3848 (2001). doi: 10.1063/1.1403010

42. D. Townsend, M. P. Minitti and A. G. Suits, “Direct current slice imaging”, Rev. Sci. Instrum. 74, 2530 (2003). doi: 10.1063/1.1544053

43. J. J. Lin, J. Zhou, W. Shiu and K. Liu, “Application of time-sliced ion velocity imaging to crossed molecular beam experiments”, Rev. Sci. Instrum. 74, 2495 (2003). doi: 10.1063/1.1561604

44. B.-Y. Chang, R. C. Hoetzlein, J. A. Mueller, J. D. Geiser and P. L. Houston, “Improved two-dimensional product imaging: The real-time ion-counting method”, Rev. Sci. Instrum. 69, 1665 (1998). doi: 10.1063/1.1148824

45. W. Li, S. D. Chambreau, S. A. Lahankar and A. G. Suits, “Megapixel ion imaging with standard video”, Rev. Sci. Instrum. 76, 063106 (2005). doi: 10.1063/1.1921671g

46. J. L. Wiza, “Microchannel plate detectors”, Nucl. Instrum. Meth. 162, 587, (1979). doi: 10.1016/0029-554X(79)90734-1

47. V. J. H. Barnes and G. M. Hieftje, “Recent advances in detector-array technology for mass spectrometry”, Int. J. Mass Spectrom. 238, 33, (2004). doi: 10.1016/j.ijms.2004.08.004

48. C. Vallance, M. Brouard, A. Lauer, C. S. Slater, E. Halford, B. Winter, S. J. King, J. W. L. Lee, D. E. Pooley, I. Sedgwickc, R. Turchetta, A. Nomerotski, J. J. John and L. Hill, “Fast sensors for time-of-flight imaging applications”, Phys. Chem. Chem. Phys. (2013). doi: 10.1039/C3CP53183J

49. N. Mirsaleh-Kohan, W. D. Robertson and R. N. Compton, “Electron ionization time-of-flight mass spectrometry: Historical review and current applications”, Mass Spectrom. Rev. 27, 237 (2008). doi: 10.1002/mas.20162

50. T. D. Märk, Electron Impact Ionization, Springer Verlag, 1985.

51. N. P. Lockyer and J. C. Vickerman, “Single Photon Ionisation Mass Spectrometry Using Laser-Generated Vacuum Ultraviolet Photons”, Laser Chem. 17, 139 (1997). doi: 10.1155/1997/53174

52. D. J. Butcher, “Vacuum Ultraviolet Radiation for Single-Photoionization Mass Spectrometry: A Review”, Microchem. J. 62, 354 (1999). doi: 10.1006/mchj.1999.1745

53. L. Hanley and R. Zimmermann, “Light and Molecular Ions: The Emergence of Vacuum UV Single-Photon Ionization in MS”, Anal. Chem. 81, 4174 (2009). doi: 10.1021/ac8013675

54. T. Imasaka, “Gas chromatography/multiphoton ionization/time-of-flight mass spectrometry using a femtosecond laser”, Anal. Bioanal. Chem. 405, 6907 (2013). doi: 10.1007/s00216-013-6960-8

55. U. Boesl, R. Weinkauf, C. Weickhardt and E. Schlag, “Laser ion sources for time-of-flight mass spectrometry,” *Int. J. Mass Spectrom. Ion Proc.,* **131**, 87 (1994). soi: 10.1016/0168-1176(93)03890-X

56. K. W. D. Ledingham and R. P. Singhal, “High intensity laser mass spectrometry - a review,” *Int. J. Mass Spectrom. Ion Proc.*, **163**, 149 (1997). doi: 10.1016/S0168-1176(97)00015-3

57. C. Weickhardt, F. Moritz and J. Grotemeyer, “Multiphoton ionization mass spectrometry: principles and fields of application,” *Eur. Mass Spectrom.*, **2**, 151(1996). doi: 10.1255/ejms.66

58. C. Koster and J. Grotemeyer, “Single-photon and multi-photon ionization of infrared laser-desorbed biomolecules,” *Org. Mass Spectrom.*, **27**, 463 (1992). doi: 10.1002/oms.1210270418

59. O. Kelly, M. J. Duffy, R. B. King, L. Belshaw, I. D. Williams, J. Sá, C. R. Calvert and J. B. Greenwood, “Femtosecond lasers for mass spectrometry: Proposed application to catalytic hydrogenation of butadiene”, Analyst 137, 64 (2012). doi: 10.1039/c1an15706j

60. M. J. Duffy, O. Kelly, C. R. Calvert, R. B. King, L. Belshaw, T. J. Kelly, J. T. Costello, D. J. Timson, W. A. Bryan, T. Kierspel, I. C. E. Turcu, C. M. Cacho, E. Springate, I. D. Williams and J. B. Greenwood, “Fragmentation of neutral Amino Acids and Small Peptides by Intense, Femtosecond Laser Pulses”, J. Am. Soc. Mass Spectrom. 24, 1366 (2013). doi: 10.1007/s13361-013-0653-6

61. J. Aoki, H. Hazama and M. Toyoda, “Novel ion extraction method for imaging mass spectrometry,” *J. Mass Spectrom. Soc. Jpn.*, **59**, 57 (2011).

62. B. Winter, E. Halford and M. Brouard, “Velocity corrected ion extraction in microscope mode imaging mass spectrometry”, submitted to Int. J. Mass Spectrom. (2013).

63. M. Lampton, O. Siegmund and R. Raffanti, “Delay line anodes for microchannel-plate spectrometers”, Rev. Sci. Instrum. 58, 2298 (1987). doi: 10.1063/1.1139341

64. M. Krems, J. Zirbel, M. Thomason and R. D. DuBois, “Channel electron multiplier and channelplate efficiencies for detecting positive ions”, Rev. Sci. Instrum. 76, 093305 (2005). doi: 10.1063/1.2052052

65. S. Matoba, R. Takahashi, C. Io, T. Koizumi and H. Shiromaru, “Absolute Detection Efficiency of a High-Sensitivity Microchannel Plate with Tapered Pores”, Jpn. J. Appl. Phys. 50, 112201 (2011). doi: 10.1143/JJAP.50.112201

66. S. Matoba, R. Takahashi, C. Io, T. Koizumi and H. Shiromaru, “Measurement of the absolute sensitivity of a high-sensitivity microchannel plate”, J. Phys.: Conf. Ser. 388, 142018 (2012). doi: 10.1088/1742-6596/388/14/142018

67. H. L. Offerhaus, C. Nicole, F. Lépine, C. Bordas, F. Rosca-Pruna and M. J. J. Vrakking, “A magnifying lens for velocity map imaging of electrons and ions”, Rev. Sci. Instrum. 72, 3245 (2001). doi: 10.1063/1.1386909

68. Y. Zhang, C.-H. Yang, S.-M. Wu, A. van Roij, W. J. van der Zande, D. H. Parker and X. Yang, “A large aperture magnification lens for velocity map imaging”, Rev. Sci. Instrum. 82, 013301 (2011). doi: 10.1063/1.3505491

69. J. H. Jungmann and R. M. A. Herren, “Detection systems for mass spectrometry imaging: A perspective on novel developments with a focus on active pixel detectors”, Rapid Commun. Mass Spectrom. 27, 1 (2013). doi: 10.1002/rcm.6418

70. J. H. Jungmann and R. M. A. Heeren, “Emerging technologies in mass spectrometry imaging”, J. Proteom. 75, 5077 (2012). doi: 10.1016/j.jprot.2012.03.022

71. X. Llopart, M. Campbell, R. Dinapoli, D. S. Segundo and E. Pernigotti, “Medipix2: A 64-k pixel readout chip with 55-μm square elements working in single photon counting mode”, IEEE Trans. Nucl. Sci. 591, 151 (2002). doi: 10.1109/TNS.2002.803788

72. X. Llopart, R. Ballabriga, M. Campbell, L. Tlustos and W. Wong, “Timepix, a 65k programmable pixel readout chip for arrival time, energy and/or photon counting measurements”, Nucl. Instr. Meth. A 581, 485 (2007). doi: 10.1016/j.nima.2007.08.079

73. A. Nomerotski, M. Brouard, E. Campbell, A. Clark, J. Crooks, J. Fopma, J. J. John, A. J. Johnsen, C. Slater, R. Turchetta, C. Vallance, E. Wilman and W. H. Yuen, “Pixel Imaging Mass Spectrometry with fast and intelligent Pixel detectors”, J. Inst. 5, C07007 (2010). doi: 10.1088/1748-0221/5/07/C07007

74. J. H. Jungmann, L. MacAleese, R. Buijs, F. Giskes, A. de Snaijer, J. Visser, J. Visschers, M. J. J. Vrakking and R. M. A. Heeren, “Fast, High Resolution Mass Spectrometry Imaging Using a Medipix Pixelated Detector”, J. Am. Soc. Mass Spectrom. 21, 2023 (2010). doi: 10.1016/j.jasms.2010.08.014

75. J. H. Jungmann, A. Gijsbertsen, J. Visser, J. Visschers, R. M. A. Herren and M. J. J. Vrakking, “A new imaging method for understanding chemical dynamics: Efficient slice imaging using an in-vacuum pixel detector”, Rev. Sci. Instrum. 81, 103112 (2010). doi: 10.1063/1.3489890

76. J. H. Jungmann, L. MacAleese, J. Visser, M. J. J. Vrakking and R. M. A. Herren, “High Dynamic Range Bio-Molecular Ion Microscopy with the Timepix Detector”, Anal. Chem. 83, 7888, (2011). doi: 10.1021/ac2017629

77. M. Brouard, E. Halford, A. Lauer, C. S. Slater, B. Winter, W. H. Yuen, J. J. John, L. Hill, A. Nomerotski, A. Clark, J. Crooks, I. Sedgwick, R. Turchetta, J. W. L. Lee, C. Vallance and E. Wilman, “The application of the fast, multi-hit, pixel imaging mass spectrometry sensor to spatial imaging mass spectrometry”, Rev. Sci. Instrum. 83, 114101 (2012). doi: 10.1063/1.4766938

78. M. Froesch, S. L. Luxembourg, D. Verheijde and R. M. A. Heeren, “Imaging mass spectrometry using a delay-line detector”, Eur. J. Mass Spectrom. 16, 35 (2010). doi: 10.1255/ejms.1052

79. W. S. Hopkins, M. L. Lipciuc, S. H. Gardiner and C. Vallance, “RG+ formation following photolysis of NO–RG via the A–X transition: A velocity map imaging study”, J. Chem. Phys. 135, 034308 (2011). doi: 10.1063/1.3610415

80. S. H. Gardiner, T. N. V. Karsili, M. L. Lipciuc, E. Wilman, M. N. R. Ashfold and C. Vallance, “Fragmentation dynamics of the ethyl bromide and ethyl iodide cations: a velocity-map imaging study,” *Phys. Chem. Chem. Phys*., published online 26 November 2014. doi: 10.1039/C3CP53970A

81. P. L. Houston, “Vector Correlations in Photodissociation Dynamics”, J. Phys. Chem. 91, 5388 (1987). doi: 10.1021/j100305a003

82. T. D. Märk, “Cross section for single and double ionization of N_2 and O_2 molecules by electron impact from threshold up to 170 eV”, J. Chem. Phys. 63, 3731 (1975). doi: 10.1063/1.431864

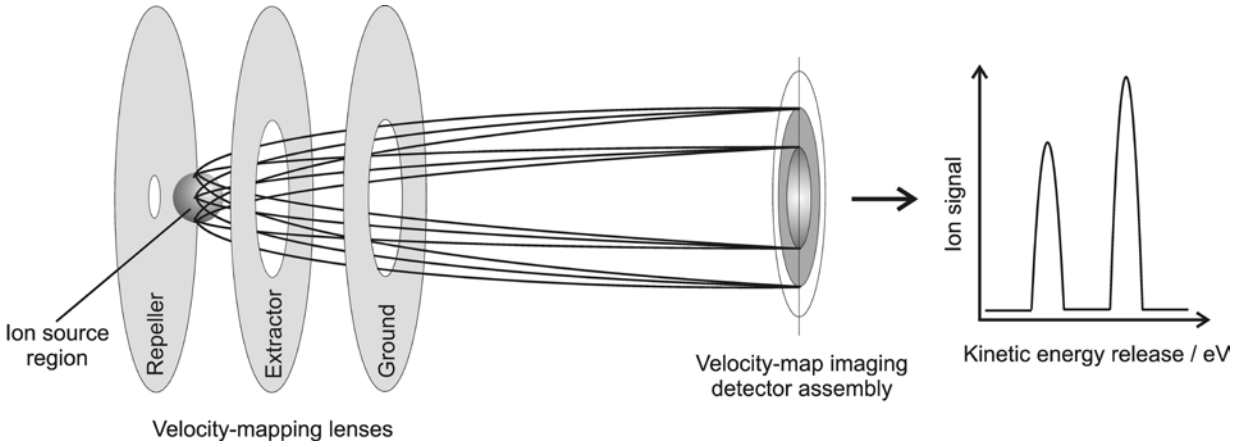

Figure 1: Schematic illustrating the operating principle of ToF velocity-map imaging. The figure illustrates velocity-mapping trajectories of a distribution of ions containing four velocities and two non-zero kinetic energy releases. The kinetic energy release distribution is acquired by integrating the velocity-map image over the angular coordinate. See text for more details.

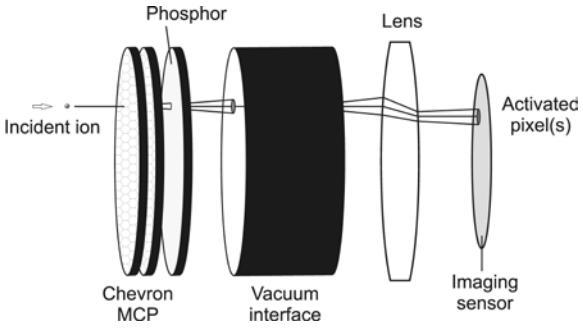

Figure 2: Exploded view of a velocity-map imaging detector assembly. Incident ions are converted into electron bursts by a chevron pair of MCPs. The electrons are incident on a phosphor screen, and the emitted light is imaged by a pixel imaging sensor.

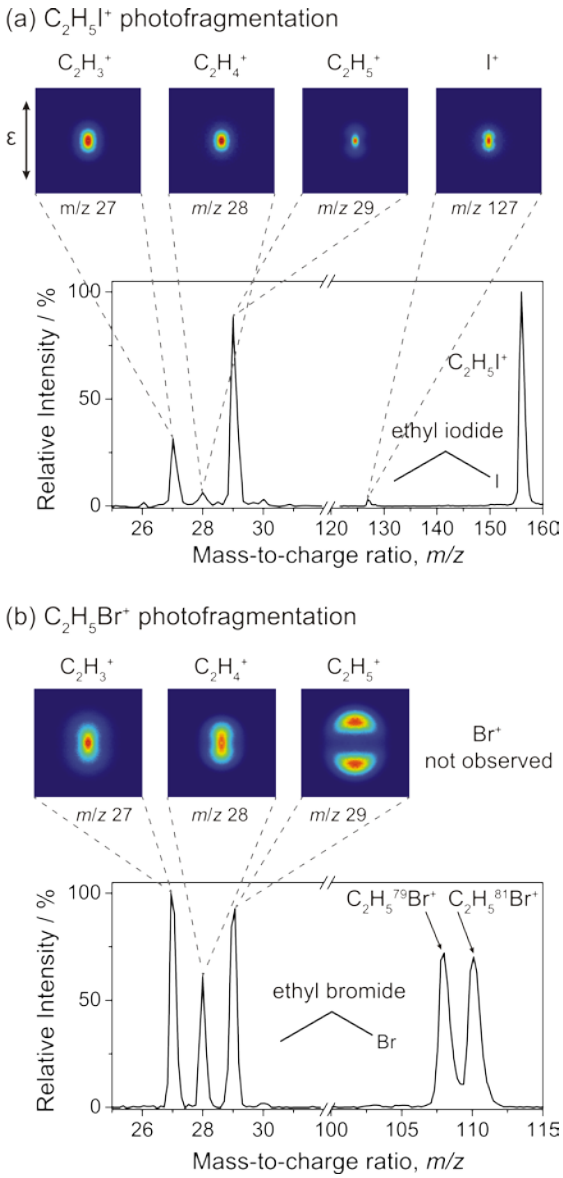

Figure 3. Mass spectra and corresponding velocity-map images for major ion fragments produced following photoionization at 118 nm and subsequent dissociation at 355 nm of (a) C_2H_5I and (b) C_2H_5Br.

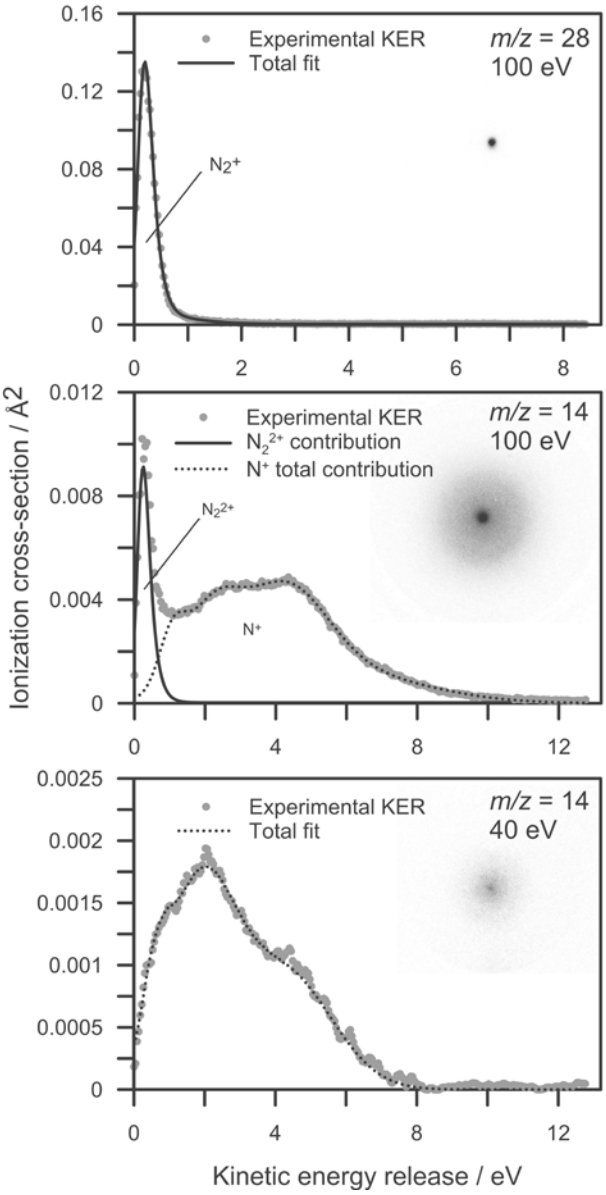

Figure 4. Fragment ion kinetic energy release distributions, normalized to the relevant partial ionization cross-section for 100 eV and 40 eV electron-impact ionization of N_2 molecules. The upper plot shows the KER profile for m/z = 28 N_2^+ (parent). The middle plot shows KER profile for m/z = 14, which contains contributions from both N_2^{2+} and N^+. The lower plot shows the N^+ KER profile from 40 eV electron impact; this electron energy is below the double ionization threshold.

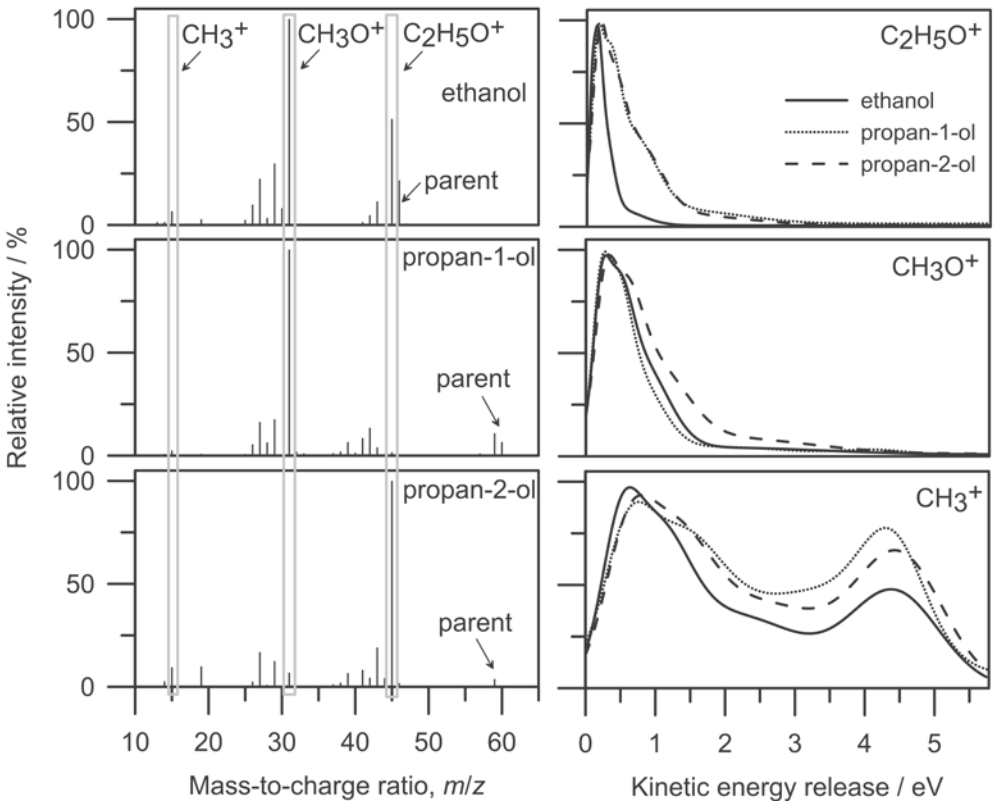

Figure 5. Left: Electron impact mass spectra for ethanol, propan-1-ol and propan-2-ol. Right: Corresponding kinetic energy release distributions extracted from velocity-map images for the $C_2H_5O^+$, CH_3O^+ and CH_3^+ ions.